Operations of DFIG with simplified rotor current reference model and solution to the recent grid code requirements

A.P. Tennakoon[1], A. Arulampalam[2], H.Leite[3], J.B. Ekanayake[4], S.G. Abeyratna[5]
[1, 2, 4 and 5]Department of Electrical and Electronic Engineering, University of Peradeniya, Peradeniya, Sri Lanka
[3]Department of Electrical and Computer Engineering, Faculdade de Engenharia da Universidade do Porto, Portugal
[1]ceprotmc@yahoo.com, [2]atpu@ee.pdn.ac.lk, [3]hleite@fe.up.pt, [4]jbe@ee.pdn.ac.lk, [5]sunil@ee.pdn.ac.lk,

***Abstract*- The advancing technologies are boosting the wind turbine development rapidly and today the wind power generation has become a proven technology. However, still the research and development are motivated to go into further detail to simplify and optimize the control strategies.**

This paper addresses a simplified control strategy based on rotor current reference frame. The decoupled active and reactive power control with decoupled movement of the operating point on its characteristics graphs such as torque slip curves is explained in detail. Further new control for DFIG operation is discussed with simulation. The simulation results have opened up explanation for its detailed operation. It has proven excellent tracking operation based on rotor current reference frame.

I. INTRODUCTION

Increase of wind power penetration into the grid network and its operational challenges has made more optimized grid codes. Today the wind farm connections and its continuous operation need to be secured by plant operators. In some cases, voltage support is also required to be satisfied up to some extend [1 and 2]. The variable speed wind turbine generators are found as the technologies of choice to satisfy these requirements. In the last decade Doubly Fed Induction Generators (DFIG) were extensively installed. Issues related to maximum power tracking, power quality, fault ride through, mechanical stress and reactive power compensation are documented [3, 4, 5, 6, 7 and 8]. Some have reported about the limitations of DFIG based wind farms on HVAC networks [9].

Further research has shown that a smooth fault ride through requirement and continuous reactive power compensation can be achieved for the large wind farm by connecting through VSC HVDC link [10, 11, 12, 13 and 14]. In the event of a fault, power from the wind farm has to be reduced either by de-loading the generator or blocking the power at the offshore converter [15 and 16]. In addition to transferring active power, the onshore converter is controlled to supply reactive power according to the Grid Code.

This paper addresses DFIG wind farm operations and its limitations on rotor side converter controls. Active and reactive power of the rotor circuit was controlled to change the rotor speed and the stator reactive power respectively. In this analysis, required active and reactive power was determined based on the rotor current vector frame. This has simplified the analysis. It demonstrated the direct decoupled real and reactive power control rather through conventional d-q frame model, which made decouple control by subtracting the dependant components in its equations.

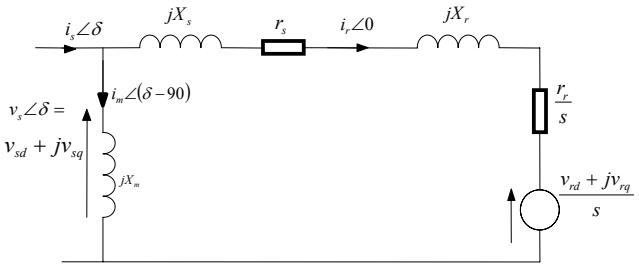

Figure 1: Simplified equivalent circuit of a DFIG

II. SIMPLIFIED MATHEMATICAL MODEL OF A DFIG TO ANALYSE LIMITATION ON ITS ROTOR CONTROL

Figure 1 shows a simplified equivalent circuit of the DFIG used to analysis its steady state operations. The voltage drop across the stator impedance is small; therefore the magnetizing reactance (x_m) is placed at the stator terminals. Motor sign convention is used for the direction of the voltages and currents. Rotor current vector is taken as the reference axis. Injected rotor voltage component (v_{rd}) is in phase with the rotor current, which represents the active power output of the rotor circuit. Injected rotor voltage component (jv_{rq}) is leading the rotor current by 90°, therefore this represents the reactive power output of the rotor circuit.

$$v_s\angle\delta = \left[i_r\left(r_s+\frac{r_r}{s}\right)+\frac{v_{rd}}{s}\right]+j\left[i_r\left(x_s+x_r\right)+\frac{v_{rq}}{s}\right] \quad --(1)$$

$$\left[\left(r_s+\frac{r_r}{s}\right)^2+\left(x_s+x_r\right)^2\right]i_r^2+\left[\left(r_s+\frac{r_r}{s}\right)v_{rd}+\left(x_s+x_r\right)v_{rq}\right]\frac{2\cdot i_r}{s}+\frac{v_{rd}^2+v_{rq}^2}{s^2}-v_s^2=0 \quad --(2)$$

The stator voltages and the currents are related by Equation 1. By equating real and imaginary components, Equation 2 is derived to calculate the rotor current. To obtain real values for the rotor currents the below condition must be satisfied:

$$v_s \geq \frac{\left|\left(r_s + \frac{r_r}{s}\right)\frac{v_{rq}}{s} - \left(x_s + x_r\right)\frac{v_{rd}}{s}\right|}{\sqrt{\left(r_s + \frac{r_r}{s}\right)^2 + \left(x_s + x_r\right)^2}} --(3)$$

In the case of low slip operating conditions, r_r/s gets high value. Therefore this condition can be simplified to:

$$v_s \geq \left|\frac{v_{rq}}{s} - \frac{\left(x_s + x_r\right)}{r_r} v_{rd}\right| --(4)$$

Equation (4) shows that the limitation on the magnitudes of the real and reactive power voltage components at lower slip operation. The rotor current also gets low values. This proves that the DFIG cannot be supported to have enough reactive power through its rotor at low slip region and when no active power injection is required.

III. RESULTS OF THE DFIG THEORITICAL ANALYSIS ON ROTOR ACTIVE AND REACTIVE POWER INJECTION

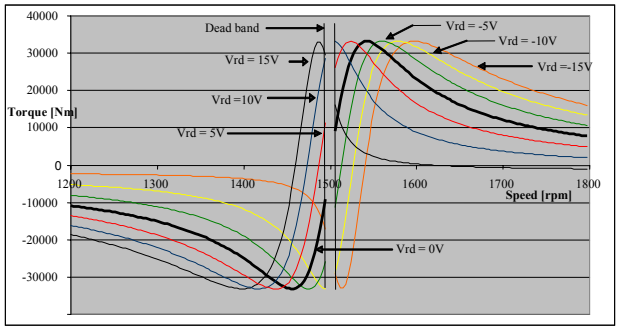

Figure 2: Torque vs speed curves of the DFIG with only different rotor active power injections

Figure 2 shows the torque slip curves when rotor voltage component v_{rd} was changed while keeping v_{rq} at zero. This graph shows that if only active power is varied through rotor injection, the torque slip curves can be shifted horizontally with the generator speed. It also clearly shown that if only active power is injected then it will not change the peak values of the curves.

Figure 3 shows the torque slip curves when rotor voltage component v_{rq} was changed while keeping v_{rd} at 10V. This shows that the torque slip curve moves vertically when only reactive power is injected through rotor circuit. Also it has proven same as in equation 4, that the reactive power injection is having limitation when less active power is injected through rotor circuit.

Further when trying to inject more reactive power the torque slip curve goes down thus the pull out torque in generator region goes down. This shows clearly low stability as operating point moves closer to pull out torque if more reactive power is injected. As a result this study results has confirmed that the real power control can be used to shift the curve horizontally while the reactive power control shifts the curve vertically.

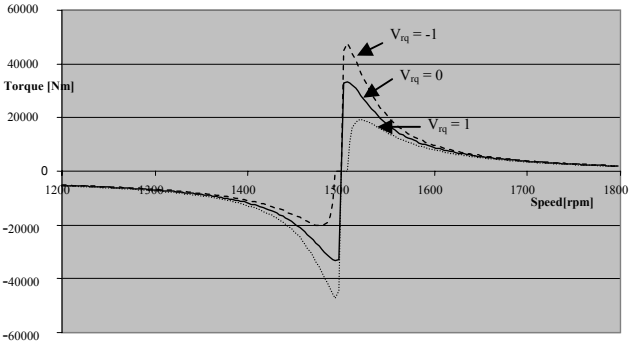

Figure 3: Torque vs speed curves of the DFIG with only different rotor reactive power injections

IV. DFIG CONTROL TECHNIQUE

a) Rotor converter basic control

Figure 4 shows rotor current Phase Lock Loop (PLL). Magnitude of the normalized q-axis current is added with the slip frequency to determine the PLL frequency. Once the PLL is synchronized it operates at slip frequency. Therefore at synchronized condition q-axis rotor current will be zero. As a result the PLL give the rotor current vector angle.

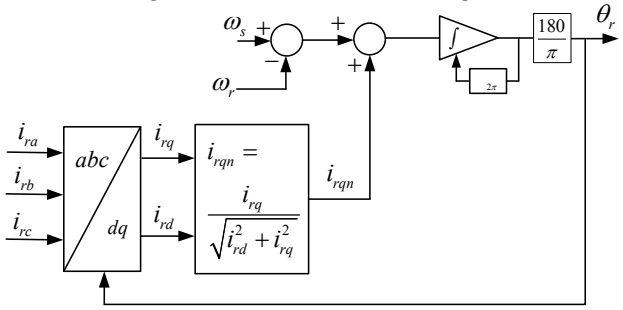

Figure 4: Rotor current vector PLL

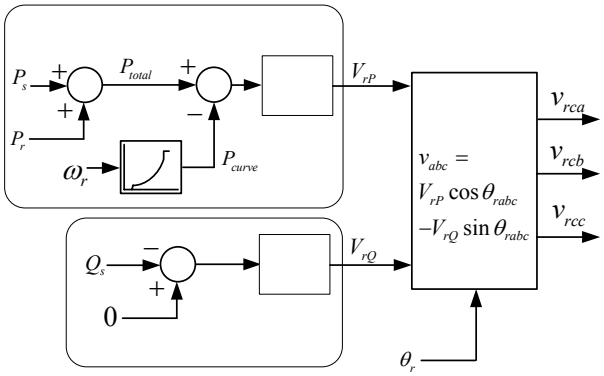

Figure 5: Active and reactive power control of the rotor converter

Figure 5 shows the active and reactive power control of the rotor converter. The maximum possible power (P_{curve}) at the generator speed is obtained from a lookup table. Total DFIG

active power output (P_{total}) is compared with the P_{curve}. The error is regulated by a PI controller to obtain the required peak voltage that need to be injected. This voltage component is injected in phase with the rotor current thus varies the active power injection. Hence the generator speed is varied until $P_{curve} = P_{total}$.

The stator reactive power, which is measured just before the stator converter connection point towards stator, is regulated to zero value through a PI controller. Hence the voltage component that is injected 90^o leading with rotor current vector varies the rotor reactive power injection in order to maintain the unity power factor at the stator terminals of the machine.

As a result the rotor converter provides independent active and reactive power control techniques, which varies generator speed while maintaining the unity power factor at the stator terminals.

b) Stator converter basic control

Figure 6 shows stator side converter control. Stator terminal three phase voltage is fed to a voltage vector PLL and thus gives the voltage vector angle. Converter dc link voltage is compared with its reference value and the error is regulated through a PI controller. This gives required active power current component, which is injected in phase with the voltage vector. This varies the active power injection from the converter and the dc link voltage is maintained.

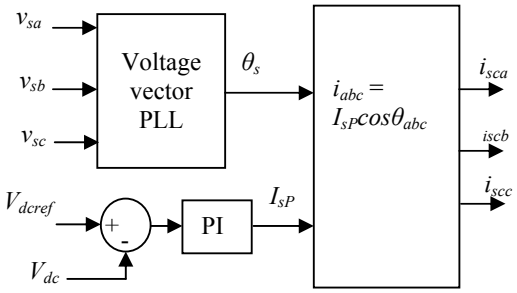

Figure 6: Stator side converter control

c) De-loading concept of the DFIG

In the event of a grid terrestrial fault, power transfer capability of the faulted network is reduced. Therefore it is necessary to reduce the wind farm output power. Active power of the rotor was controlled to shift the torque slip curve to right side (Figure 2). This brings the generator operating point closer to zero torque operation. This reduces the generator torque and hence reduces the generator output power to match with the transferable electrical power of the network. This can be achieved by adding an active power voltage component (V_{rp_Deload}) together with the output of the rotor active power control voltage (V_{rp}) shown in Figure 5.

The de loading control is shown in Figure 7. Here q-axis voltage component of the stator terminal is given as input to the PI controller. The PI controller regulates this voltage to be zero by adjusting rotor active power de-loading voltage component.

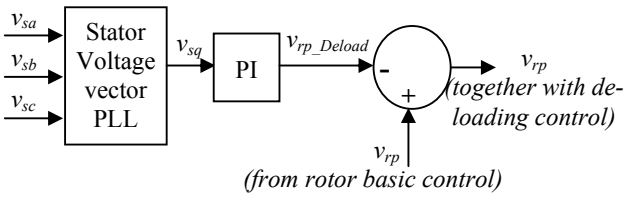

Figure 7: Rotor active power control together with the de-loading control

When there is a ground fault, the stator voltage frequency will try to increase as the grid network is unable to transfer power at low voltage conditions. Even though the stator voltage vector PLL tries to lock the voltage vector, it will fail due to continuous frequency increase. As a result this will introduce a q-axis voltage. This component will be decreasing the resultant rotor voltage injection that is related to active power and shifts the torque slip curve towards high rotor speed side. As this controller response (shifting speed) is faster than the increase in mechanical speed, the electrical torque will be reduced and thus the machine will be de-loaded.

d) Stator side reactive power control to support grid network voltage according to the recent grid code requirement

Maintaining the grid network voltage is addressed as one of the issues in the recent grid codes. Also during low slip operation and low active power injection period the reactive power control through rotor injection has some limitation. Therefore the grid side network voltage can be controlled by the stator side converter. Especially it helps when there is low active power injection made by the rotor converter. Measured grid voltage is regulated through a PI controller and its output I_{sQ} will be inserted in the current calculation shown in Figure 6 using equation 5.

$$i_{sc\_abc} = I_{sP} \cos\theta_{abc} + I_{sQ} \sin\theta_{abc} \quad --(5)$$

V. COMPARISON WITH EXISTING DFIG COTROLERS

Most of the existing DFIG controller models are designed in the stator voltage or flux oriented reference frame. These controllers consist of machine parameter dependant cross coupling terms to have independent rotor injection control of active and reactive power [9]. Therefore if the machine parameters are not properly incorporated in the controller there could be errors in the output which can not be corrected by a simple PI controller. The Rotor current reference frame does not have cross coupling terms and hence the controller is simplified and fully independent of machine parameters. The power system transient effects to the rotor side are less compared to the stator side as the rotor and the stator are mutually coupled magnetically. Hence the transient disturbances to the Phase Locked Loop (PLL) to track rotor angle is less when rotor reference frame is used.

VI. SIMULATION RESULTS AND DISCUSSION

The controller explained in Figures 4 and 5 was simulated using EMTDC/PSCAD simulation package. A 60 MW wind farm was modeled using lumped DFIG generator model (refer Appendix) and observed excellent performance in tracking.

Figures 8 and 9 show the simulation results. Initially the rotor controller was engaged to get stabilized by synchronizing its PLL to the system while rotor injection was blocked. This initial part results show clearly the DFIG operation without rotor injection.

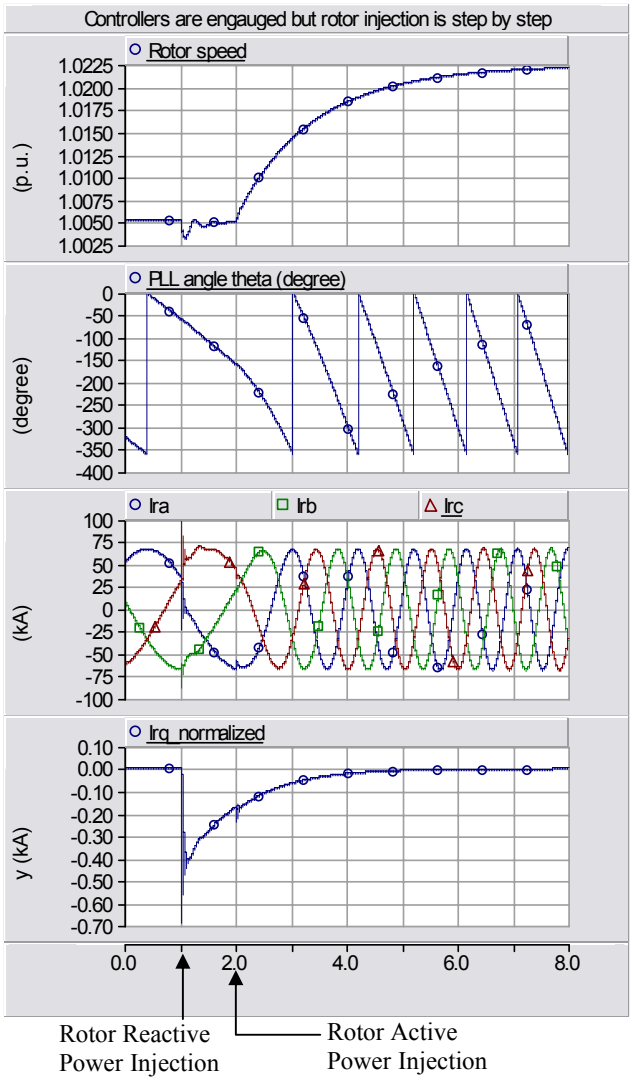

Figure 8: Simulation result: at 1 second rotor reactive power injection and at 2 seconds rotor active power injection were activated

The rotor injection was engaged step by step. Initially the stator terminal reactive power control was engaged at 1 second. It can be seen very clearly from 1st graph in Figure 9 that immediately after its injection the stator terminal reactive power consumption has changed to zero. This shows the rotor reactive power control to maintain unity power factor operation at the stator terminal with very small reactive power injection from the rotor.

Further the rotor active power injection was engaged at 2 seconds. The last graph of Figure 9 shows that the wind farm output power (P_{wind_farm}) is same as the power taken from the look up table ($P_{look\ up\ table}$) at that specific speed of the rotor, which is a fast action and achieved by shifting the torque slip curve. As a result during the transient period, the wind farm output power got reduced. Due to the miss match between the out put power and input power, the turbine speed increased and finally the operating point moved towards stable operation at a higher output power. Here, this response is slow as it needs to go through the inertia constant of the turbine. This slow response has a good effect on the operation of the DFIG as it smoothens out the wind farm output power due to fluctuation in input wind power.

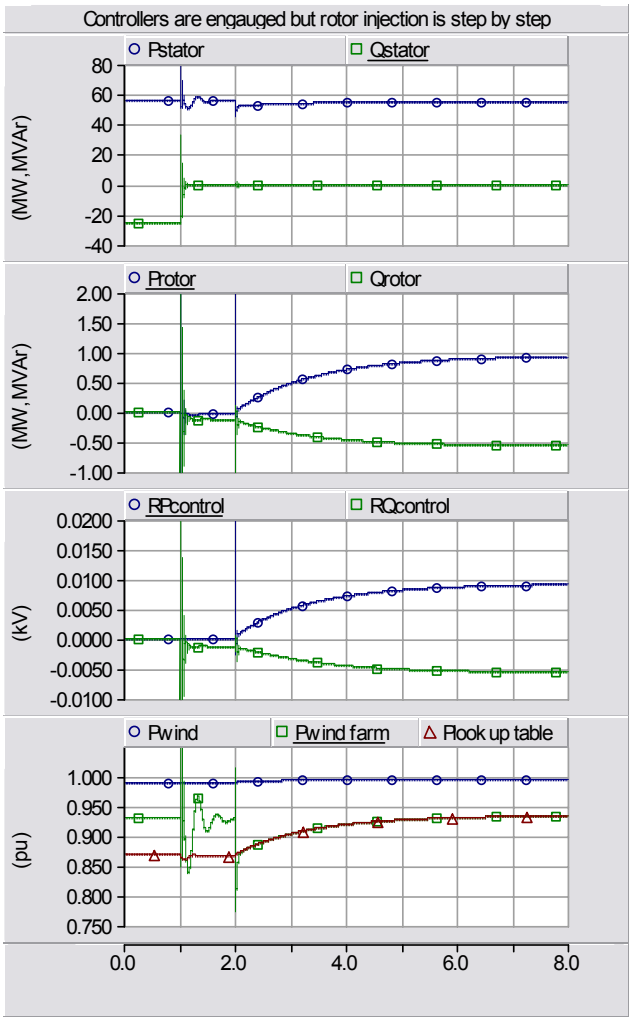

Figure 9: Simulation result: at 1 second rotor reactive power injection and at 2 seconds rotor active power injection were activated

At the steady state operation of the wind farm with the rotor control, the wind farm output power increased to 0.935

pu. This was due to rotor control. Further the power extracted from the wind by the turbine also increased to 0.995 pu. This is due to the increase in turbine speed up to 1.022 pu which is the maximum power extraction operating point at 11.5 m/s wind speed.

VII. CONCLUSION

A simplified rotor frame DFIG model is discussed with decoupled rotor active and reactive power injection. The DFIG steady state operation is clearly explained with its torque slip curve in terms of its rotor active and reactive power injection. Finally a new rotor current vector based control is proposed for the DFIG operations. It was simulated and the results have been shown and discussed in detail with their transient response. This has proven that the proposed control performed excellently (i) for the rotor reactive power control on stator terminal unity power factor operation and (ii) the rotor active power control on maximum power curve traction of the DFIG.

ACKNOWLEDGMENT

The authors acknowledge Professor Nick Jenkins from Cardiff University, UK and Mr. G. Ramtharan from Garrad Hassan industry, UK for their support to this research work. Also our sincere thanks for the National Science Foundation in Sri Lanka for their research grant (RG/2006/W&E/01) support to carryout this work at University of Peradeniya, Sri Lanka.

REFERENCES

[1] National Grid Electricity Transmission - UK "The Grid Code", *Issue 3, Revision 19, United Kingdom, 1st January 2007, Website: http://www.nationalgrid.com/uk/Electricity/Codes/gridcode/gridcodedocs/, accessed May 2007.*

[2] E.ON Netz GmbH, Bayreuth, "Grid Code – High and extra high voltage", *1st April 2006, Website: http://www.eon-netz.com/EONNETZ_eng.jsp, links to "Grid utilization" → "Grid connection regulations", accessed May 2007.*

[3] S. Muller, M. Deicke and R.W. De Doncker, "Doubly fed induction generator systems for wind turbines", *IEEE Industry Application Magazine, Volume 8, Issue 3, pp 26 – 33, May-June 2002.*

[4] Lie Xu and P. Cartwright, "Direct active and reactive power control of DFIG for wind energy generation", *IEEE Transactions on Energy Conversion, Volume 21, Issue 3, pp 750 – 758, Sept. 2006.*

[5] P. Cartwright, L. Holdsworth, J.B. Ekanayake and N. Jenkins, "Co-ordinated voltage control strategy for a doubly-fed induction generator (DFIG)-based wind farm", *IEE Proceedings Generation, Transmission and Distribution, Volume 151, Issue 4, pp 495 – 502, Jul 2004.*

[6] F.M. Hughes, O. Anaya Lara, N. Jenkins and G. Strbac, "Control of DFIG-based wind generation for power network support", *IEEE Transactions on Power Systems, Volume 20, Issue 4, pp 1958 – 1966, Nov. 2005.*

[7] D. Xiang, L. Ran, J.R. Bumby, P.J. Tavner and S. Yang, "Coordinated Control of an HVDC Link and Doubly Fed Induction Generators in a Large Offshore Wind Farm", *IEEE Transactions on Power Delivery, Volume 21, Issue 1, pp 463 – 471, Jan. 2006.*

[8] Bossanyi Ervin, "Wind turbine control for load reduction", *Wind Energy, Volume 6, pp 229 – 244, 2003.*

[9] A.P. Tennakoon, A. Arulampalam, J.B. Ekanayake, S.G. Abeyratne and A.M.U.S.K. Alahakoon, "Operational restrictions with maximum power extraction of DFIG connected wind farms", *IEEE International Conference on Sustainable Energy Technologies (ICSET), SMU conference center, Singapore, pages 1073 – 1078, November 2008.*

[10] A. Arulampalam, G. Ramtharan, N. Caliao, J.B. Ekanayake, and N. Jenkins, *"Simulated onshore-Fault Ride Through of offshore wind farms connected through VSC HVDC", Journal of Wind Engineering, Volume 32, Issue No. 2, page 103-114, March 2008.*

[11] F. Blaabjerg, A. Consoli, J.A. Ferreira and J.D. Van Wyk, "The future of electronic power Processing and conversion", *IEEE Transactions on Power Electronics, Volume 20, Issue 3, pp 715 – 720, May 2005.*

[12] Lie Xu, and Bjarne R. Andersen, "Grid connection of Large Offshore Wind Farms Using HVDC", *Wind Energy, Volume 9, Issue 4, pp 371-382, 2006.*

[13] F. Iov, P. Sorensen, A.D. Hansen and F. Blaabjerg, "Grid connection of active stall wind farms using a VSC based DC transmission system", *European conference on Power Electronics and Applications, pp 1-10, Sept. 2005.*

[14] J.M. Carrasco, L.G. Franquelo, J.T. Bialasiewicz, E. Galvan, R.C. PortilloGuisado, M.A.M. Prats, J.I. Leon and N. Moreno-Alfonso, "Power-Electronic Systems for the Grid Integration of Renewable Energy Sources: A Survey", *IEEE Transaction on Industrial Electronics, Vol. 53, Issue 4, pp. 1002–1016, June 2006.*

[15] G. Ramtharan, A. Arulampalam, J.B. Ekanayake, F.M. Hughes and N. Jenkins, "Fault ride through of fully rated converter wind turbines with AC and DC transmission systems", *Accepted for publishing in the IET Renewable Power Generation latter part of 2008.*

[16] V. Akhmatov, "Modeling and ride-through capability of variable speed wind turbines with permanent magnet generators", *Wind Energy, Vol. 9, Issue 4, pp. 313-326, July/August 2006.*

APPENDIX

The 5th order model of the wound rotor induction machine was used for the EMTDC/PSCAD simulations

Parameters of the Machine

MVA = 60, Terminal Voltage = 690V,

Rotor Resistance = 0.00549p.u.,

Stator Resistance = 0.00488p.u.,

Stator/Rotor Mutual Inductance = 3.95279p.u.,

Stator Leakage Inductance = 0.09241p.u.,

Rotor Leakage Inductance = 0.09955p.u.

Base speed = synchronous speed;

Rotor stator turns ratio = 1 : 1,

Operating Frequency = 50Hz

System Fault Level = 2400 MVA